arXiv:1609.09429v1 [stat.AP] 29 Sep 2016

Visualizing Dependence in High-Dimensional Data: An Application to S&P 500 Constituent Data

Marius Hofert[1], Wayne Oldford[2]

2016-09-30

Abstract

The notion of a zenpath and a zenplot is introduced to search and detect dependence in high-dimensional data for model building and statistical inference. By using any measure of dependence between two random variables (such as correlation, Spearman's rho, Kendall's tau, tail dependence etc.), a zenpath can construct paths through pairs of variables in different ways, which can then be laid out and displayed by a zenplot. The approach is illustrated by investigating tail dependence in constituent data of the S&P 500 during the financial crisis of 2007–2008. The corresponding Global Industry Classification Standard (GICS) sector information is also addressed.

Zenpaths and zenplots are useful tools for exploring dependence in high-dimensional data from the realm of finance, insurance and quantitative risk management. All presented algorithms are implemented using the R package `zenplots` and all examples and graphics in the paper can be reproduced using the accompanying demo `SP500`.

Keywords
Zenpath, zenplot, detecting dependence, high dimensions, graphical tools.

MSC2010
62-09, 62H99, 65C60

1 Introduction

Motivated by the use of high-dimensional data such as data from several hundred risk-factor changes in the realm of quantitative risk management, we raise the following simple question:

> How can one detect and visualize dependence in high-dimensional data?

[1]Department of Statistics and Actuarial Science, University of Waterloo, 200 University Avenue West, Waterloo, ON, N2L 3G1, `marius.hofert@uwaterloo.ca`. The author would like to thank NSERC for financial support for this work through Discovery Grant RGPIN-5010-2015.
[2]Department of Statistics and Actuarial Science, University of Waterloo, 200 University Avenue West, Waterloo, ON, N2L 3G1, `rwoldford@uwaterloo.ca`.

Detecting and visualizing dependence in high-dimensional data is important for model building and inference in areas such as finance, insurance and quantitative risk management, where the one-period ahead behaviour of a high-dimensional portfolio represented by a random vector $\boldsymbol{X} = (X_1, \dots, X_d)$, d large, is studied; see McNeil et al. (2015, Section 2.2.1).

The example we consider in this work is that of detecting and visualizing tail dependence of a portfolio consisting of sign-adjusted log-returns of all constituents of the S&P 500, so we have realizations $(X_{t,j})_t$ of $X_j = X_{t,j} = -\log(S_{t,j}/S_{t-1,j})$, $j \in \{1, \dots, d\}$, for $d \approx 500$, and $S_{t,j}$ denotes the end-day price of constituent j of the S&P 500 at time $t \in \{1, \dots, T\}$. To each component of this high-dimensional data, we fit an $\text{ARMA}(1,1) - \text{GARCH}(1,1)$ model, extract the corresponding standardized residuals and (exemplary) investigate their tail dependence in the so-called *copula-GARCH* framework (see Patton (2006) and Patton (2013)) by considering the pseudo-observations of the standardized residuals.

The high dimensions we consider in this paper are of the order of several hundreds. Dimensionality reduction is often not a practical option when, for example, components X_j, $j \in \{1, \dots, d\}$, are each individually of interest (such as for a portfolio of life insurance contracts) and need to be tracked. Computationally, this is already fairly demanding, requiring, for example, efficient algorithms to estimate a (Student) t copula in large dimensions. Providing meaningful displays of such high dimensional output adds to this challenge.

Our running example will be the S&P 500 constituent data. The source, the time-series models we fit, and the connection with copulas, are all described in Section 2. This setup provides the high-dimensional model output that will then be visualized. Section 3 presents the zenplot, a compact graphical presentation of high-dimensional data arranged in a path of one- and two-dimensional displays. When dimensions are high it will often be necessary to draw attention to, and to display, only the most salient features of the data. To this end, Section 3.2 introduces the notion of a zenpath, a tool to provide an interesting path through the pairs of variables. All graphs in this paper can be reproduced with the demo `SP500` provided in the R package `zenplots`; see Hofert and Oldford (2016). In the last section we provide concluding remarks.

2 S&P 500 constituent data

We consider time series of all 505 constituents[3] of the S&P 500 as of 2015-10-12[4]. However, our interest lies in the 756 trading days between 2007-01-01 ($t = 0$) and 2009-12-31 ($t = T$) which contains the global financial crisis of 2007–2008. This data was downloaded from a publicly available source (`https://finance.yahoo.com/` on 2016-01-03) and then incorporated into the R package `qrmdata`; see Hofert and Hornik (2016). We assume that the order of the data is according to their Global Industry Classification Standard (GICS) information (see the demo `SP500`). Of course any company joining the S&P 500 after

[3]Note that the S&P 500 does not necessarily have exactly 500 constituents.

[4]see `https://en.wikipedia.org/wiki/List_of_S%26P_500_companies`

2009-12-31 will not appear in this period and, for the remainder there can be much data missing.

To assess the extent of the missing data, we plot in Figure 1 (left-hand side) the days

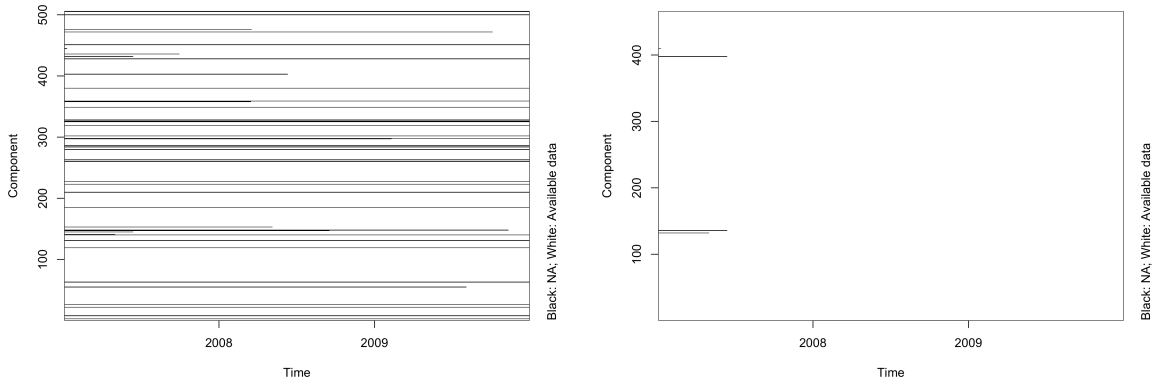

Figure 1 Missing data for all 505 S&P 500 constituents from 2007-01-01 to 2009-12-31 (left-hand side); days with missing data are marked for each constituent. We work with the 465 constituents with maximally 20% missing data (right-hand side) and fill the missing data via `na.fill(, fill = "extend")`.

missing a value for each of the 505 constituents. The missing data pattern likely indicates that many of the constituents joined the S&P 500 in this period (or after for those whose lines span the time period). We are still left with 465 companies if we retain only those having at least 80% complete data. As the right-hand side of Figure 1 shows, only four of these have any data missing. Restricting our analysis to these 465 constituents, those with missing data will be "filled", by interpolation between adjacent data where available or by extrapolation from the earliest time point back to the beginning of the series. In the end, we will work with a complete data set having $T = 756$ daily records on $d = 465$ dimensions.

2.1 Modelling the margins

We will first model the 755 negative log-returns for each of the 465 constituents. Given our time horizon and the financial crisis of 2007–2008, we cannot assume each constituent series of negative log-returns to be realizations of independent and identically distributed (iid) random variables. Instead, we need to incorporate some serial (temporal) dependence for each series. Because of the large number of marginal time series, we take a broad-brush approach and use the popular ARMA$(1,1)-$GARCH$(1,1)$ model for each margin separately (de-GARCHing).

These models have the form

$$\begin{aligned} X_{t,j} &= \mu_{t,j} + \varepsilon_{t,j} \quad \text{for} \quad \varepsilon_{t,j} = \sigma_{t,j} Z_{t,j}, \\ \mu_{t,j} &= \mu_j + \phi_j(X_{t-1,j} - \mu_j) + \theta_j(X_{t-1,j} - \mu_{t-1,j}), \\ \sigma^2_{t,j} &= \alpha_{j0} + \alpha_{j1}(X_{t-1,j} - \mu_{t-1,j})^2 + \beta_j \sigma^2_{t-1,j}, \end{aligned}$$

where, for all components $j \in \{1, \dots, d\}$, $\mu_j \in \mathbb{R}$, $|\phi_j| < 1$, $|\theta_j| < 1$, $\alpha_{j0} > 0$, $\alpha_{j1} \geq 0$, $\beta_j \geq 0$, $\alpha_{j1} + \beta_{jk} < 1$.

The stochastic component $Z_{t,j}$ for each series $j \in \{1, \dots, d\}$ are the *standardized residuals* (or *innovations*). For each series these are taken to be iid, centred about zero and have unit variance. We model the innovation distribution as a scaled (Student) t distribution; that is, for each $j \in \{1, \dots, d\}$, $Z_{t,j} \overset{\text{ind.}}{\sim} F_j(z) = t_{\nu_j}(z\sqrt{\nu_j/(\nu_j - 2)})$, where t_{ν_j} is the distribution function of the standard t distribution with ν_j degrees of freedom.

Even though each series is fit separately, the fitting itself is non-trivial for so many components. We thus use the robust `fit_ARMA_GARCH()` from `qrmtools` (developed for this purpose; see Hofert and Hornik (2015)) and `solver = "hybrid"` for the underlying fitting procedure `ugarchfit()` of `rugarch` (see Ghalanos (2011)). The appearing six warnings can safely be ignored here as they only indicate issues in finding initial values for the fitting; see the demo for more details. A residual check is presented in Figure 9 in the Appendix based on zenplots introduced in Section 3.

2.2 Modelling cross-sectional dependence

Having modelled the series marginally, we turn our attention to the multivariate series of standardized residuals $(\boldsymbol{Z}_t)_t$ for iid $\boldsymbol{Z}_t = (Z_{t,1}, \dots, Z_{t,d}) \sim H$ to model their cross-sectional dependence (that is, the contemporaneous dependence). To this end, we assume that each marginal distribution function F_j of H is continuous, $j \in \{1, \dots, d\}$.

By Sklar's Theorem, see Sklar (1959), the joint distribution function H of $\boldsymbol{Z}_t$ can be decomposed as

$$\begin{aligned} H(z_1, \dots, z_d) &= C(F_1(z_1), \dots, F_d(z_d)), \quad \boldsymbol{z} \in \mathbb{R}^d \\ &= C(u_1, \dots, u_d), \quad \boldsymbol{u} \in [0,1]^d, \end{aligned}$$

for some copula C as a function of the marginal distribution functions $F_1, \dots, F_d$ of H. In combining the marginal distribution functions $F_1, \dots, F_d$ to give H, the copula C determines the dependence between $Z_{t,1}, \dots, Z_{t,d}$. Since $u_j = F_j(z_j)$, the copula is itself a distribution function having marginal $\mathrm{U}(0,1)$ distributions.

In practice, we do not observe data from C but rather from H. The F_j are typically unknown, so we must work instead with *pseudo-observations*, to be constructed from estimates $\widehat{F}_j$ of F_j for $j \in \{1, \dots, d\}$. Parametrically estimated marginal distribution functions $\widehat{F}_1, \dots, \widehat{F}_d$ could generate the corresponding pseudo-observation via $\widehat{F}_j(Z_{t,j})$, $t \in \{1, \dots, T\}$, $j \in \{1, \dots, d\}$. However, in this case, model misspecification of the marginal

distribution functions can be a problem, one which is considerably amplified when the number of distributions to be assessed (for example, by a goodness of fit test) becomes large ($d = 465$ in our case).

Instead, the standard approach is non-parametric (for example, see Genest et al. (2009)) based on the empirical distribution functions $\widehat{F}_{T,1}, \ldots, \widehat{F}_{T,d}$ (computed from the T observations for each of d dimensions). These are corrected slightly as $\frac{T}{T+1}\widehat{F}_{T,j}(Z_{t,j})$ to avoid having any estimated value of a distribution function be exactly one. Then, for $t \in \{1, \ldots, T\}$, $j \in \{1, \ldots, d\}$ the pseudo-observations are thus equivalent to taking

$$U_{t,j} = \frac{R_{t,j}}{T+1} \tag{1}$$

where $R_{t,j}$ denotes the rank (smallest to largest) of $Z_{t,j}$ among $Z_{1,j}, \ldots, Z_{T,j}$.

The observed joint distribution of the pseudo-observations can then be used to provide insight on the copula function C and hence the underlying stationary cross-sectional dependence.

3 Visualizing dependence in high dimensions with zenplots

A scatterplot of the pseudo-observations $U_{t,j}$, $t \in \{1, \ldots, T\}$, $j \in \{1, \ldots, d\}$ can reveal a lot about the dependence structure between any pair of variates and can give some sense of what features the underlying unknown copula model has. To simplify the demonstration of this based on our S&P 500 data, consider all columns (or components) sorted according to their GICS sectors in alphabetical order (together with the number of constituents of that sector): "Consumer discretionary" (78), "Consumer staples" (33), "Energy" (36), "Financials" (85), "Health care" (51), "Industrials" (63), "Information technology" (60), "Materials" (25), "Telecommunications services" (5), and "Utilities" (29). Within each sector, the original order of the components remains untouched. From left to right, Figure 2 shows a scatterplot of independently distributed $\mathrm{U}(0, 1)$ observations followed by plots of the pseudo-observations for a few pairs of the S&P 500 constituents' residuals. If the standardized residuals from a pair of stocks are statistically independent from one another, then this plot should be indistinguishable from points uniformly distributed over the unit square as, for example, they are in the left-most scatterplot of Figure 2.

Roughly speaking, the less the pseudo-observations look like independent uniforms the stronger is their dependence. For example, each of the three right-most plots in Figure 2 departs some from a uniform, though not dramatically. Each is a little sparser in the top left and bottom right corners and is a little denser in the bottom left and top right corners. Though somewhat weak, this shows a positive (quadrant) dependence between the standardized residuals of these pairs of stocks over this period. The strongest of the three appears to be the right-most plot in Figure 2 – as one might expect between the standardized residuals of AutoNation Inc. (`AN`) and AutoZone Inc. (`AZO`).

Figure 3 displays the scatterplot matrix of the pseudo-observations of the standardized

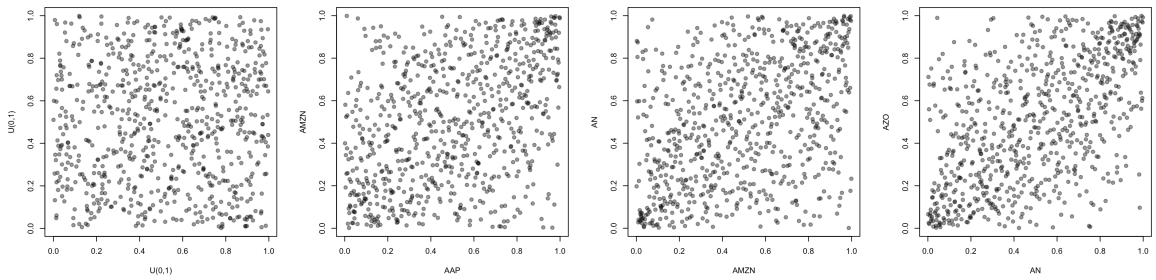

(a) $\mathrm{U}(0,1) \times \mathrm{U}(0,1)$ (b) $(U_{t,1}, U_{t,2})$ = (AAP, AMZN) (c) $(U_{t,2}, U_{t,3})$ = (AMZN, AN) (d) $(U_{t,3}, U_{t,4})$ = (AN, AZO)

Figure 2 Scatterplots of (a) independent $\mathrm{U}(0,1)$ random variables and (b, c, d) the pseudo-observation pairs $(U_{t,j}, U_{t,j+1})$, $j \in \{1,2,3\}$. Ticker symbol abbreviations: AAP = Advanced Auto Parts, AMZN = Amazon.com Inc., AN = AutoNation Inc., and AZO = AutoZone Inc.

residuals from marginally fitting the first 22 constituents of our S&P 500 data. In addition to being able to simultaneously display and compare many plots at once, the scatterplot matrix has another important characteristic when it comes to assessing dependence – it produces small scatterplots. Small scatterplots make our visual system focus on the low spatial frequency characteristics of each plot and this is ideal for detecting dependence structure from uniforms.

For example, consider again the plots of Figures 2. The right-most three plots appear in Figure 3 as the first three plots from the top left along the first diagonal above the main diagonal; that is, considering the scatterplot matrix as a 22×22 matrix, the right-most three plots of Figures 2 appear in cells $(1,2)$, $(2,3)$, and $(3,4)$, respectively, of the scatterplot matrix. Moving your eye along the first three plots of this diagonal, it is easier to see the dependence in each plot and that this dependence is increasing as the eye travels down and to the right. The same visual effect can be achieved with Figure 2 by squinting when observing the plots, or by physically moving farther away (and hence making them smaller).

Note that some care has been taken in the construction of the scatterplot matrix. No superfluous annotation appears (no axes, etc.), each point is plotted with a very small size, and the colour used for plotting includes an alpha level chosen so that overplotted points will show darker (so-called *alpha-blending*) to better visually suggest the density of the distribution.

Looking over the scatterplot matrix one can assess the (in)dependence of any pair and compare the strength of the dependence for different pairs. For example, considering only the top left 4×4 block, we can see that position $(1,4)$ shows the highest dependence in this block, with a preponderance of points in having high joint returns. This scatterplot is that of AZO and AAP and shows a stronger dependence than that of AZO and AAP shown in $(3,4)$ or the right-most plot in Figure 2. In the rest of the matrix there are other stronger, and many weaker, types of dependence that can also be seen. The dependence that stands

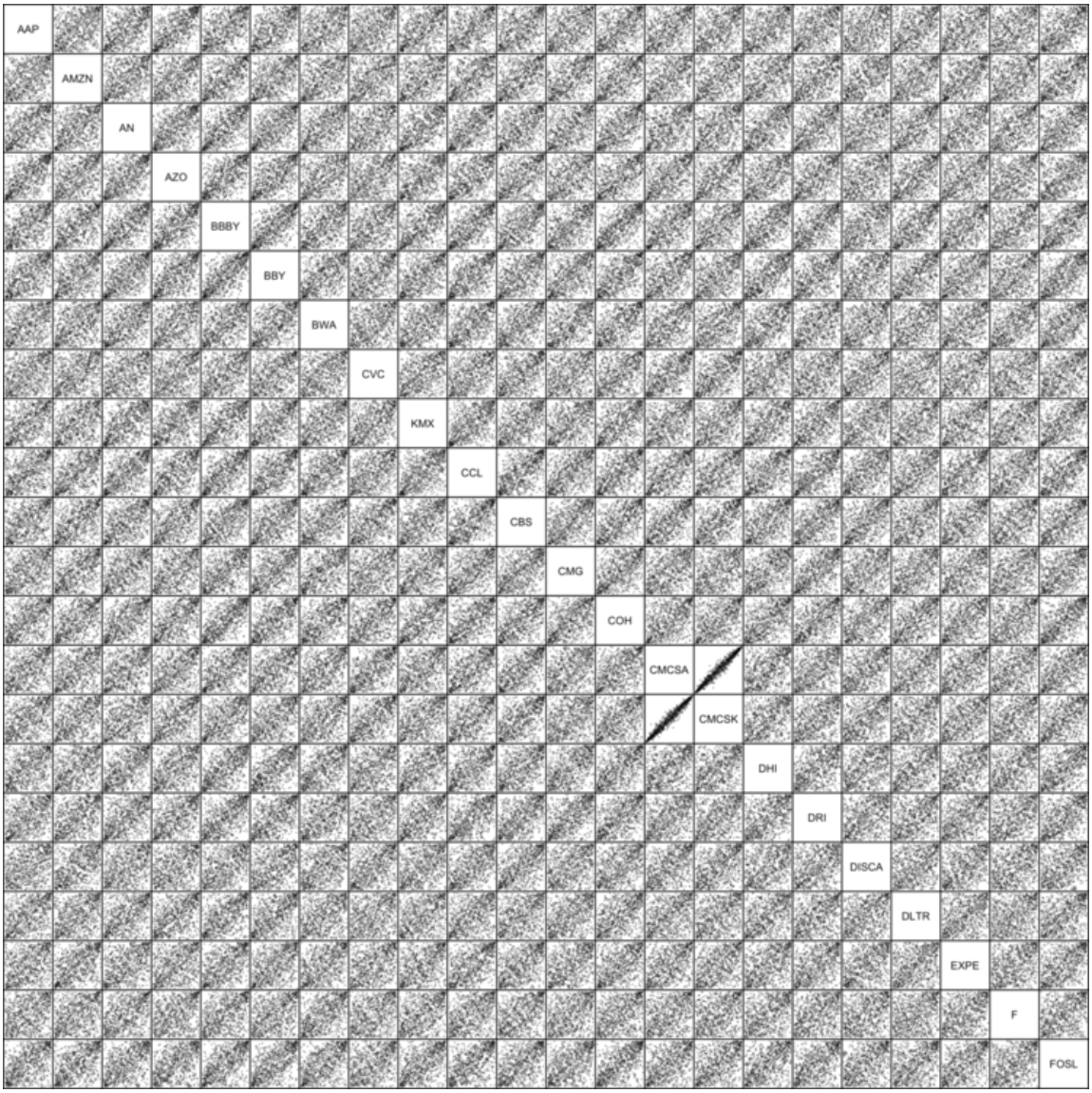

Figure 3 Scatterplot matrix of $(\boldsymbol{U}_{t,j})_t$, $j \in \{1, \ldots, 22\}$. Small displays highlight low spatial frequency structure, and hence dependence structure, and allow the dependence of many pairs to be assessed and compared simultaneously.

out most is that of `CMCSA` and `CMCSK`, near the diagonal in position $(14, 15)$. These are the pseudo-observations for the standardized residuals on two different classes of Comcast shares, which explains such a strong dependency.

3.1 Zenplots

A major drawback of the scatterplot matrix is its wasted space. Every plot appears twice, once above the main diagonal and once below – for example, the two strongest dependencies seen near the main diagonal of Figure 3 are the same pairs of Comcast constituents. In this display of 462 scatterplots, only 231 show different pairs (possibly after a rotation or reflection).

In contrast, a *zenplot* (or *zigzag expanded navigation plot*) lays out many more scatterplots by making better use of the space. The plots are laid out following a well defined path that zigzags across the page. Figure 4 shows a zenplot that displays $d - 1 = 464$ *different* scatterplots in approximately the same space; to this end we used `zenplot()` of the `R` package `zenplots`. As with the scatterplot matrix one sees two very strong dependencies. Unlike the scatterplot matrix, these are two different pairs of stocks: the one in the first row is that of the Comcast shares as before, but the one in the fourth row is a pair of two different classes of Twenty-first Century Fox shares (`FOX` and `FOXA`). The zenplot allows visual search and comparison over twice as many plots as does a scatterplot matrix in the same space; note that the labels of the pairs can be made more visible by zooming in on Figure 4.

The zenplot lays out the scatterplots as follows. The first is placed in the top left corner. This has variate 1 as its horizontal axis and variate 2 as its vertical. The next plot is placed at the right of the first with variate 2 as its vertical axis and variate 3 as its horizontal. The third scatterplot is placed below the second with variate 3 as its horizontal and variate 4 as its vertical. The next scatterplot is placed to the right of this sharing the same vertical axis and having variate 5 as its horizontal axis. Then the next plot is placed above the fourth with horizontal variate 5 and vertical variate 6. One zigzag pattern is now completed and we are in a position similar to the starting position. This continues left to right across the page until the end where the zigzag moves down and reverses its direction to be right to left. And so on until all plots have been laid out. Whenever an axis is shared, the name of that variate appears between the two plots.

If one imagines the $d \times d$ scatterplot matrix of all d variates, the zenplot of Figure 4 has plotted all scatterplots that lie along the diagonal of the scatterplot matrix immediately above the main diagonal – it plots the pairs $(1, 2), (2, 3), \ldots, (d-1, d)$. For example, the three scatterplots in the top left corner of Figure 4 are exactly the three right-most scatterplots of Figure 2. Many other customizations of zenplots are possible; see `?zenplot`.

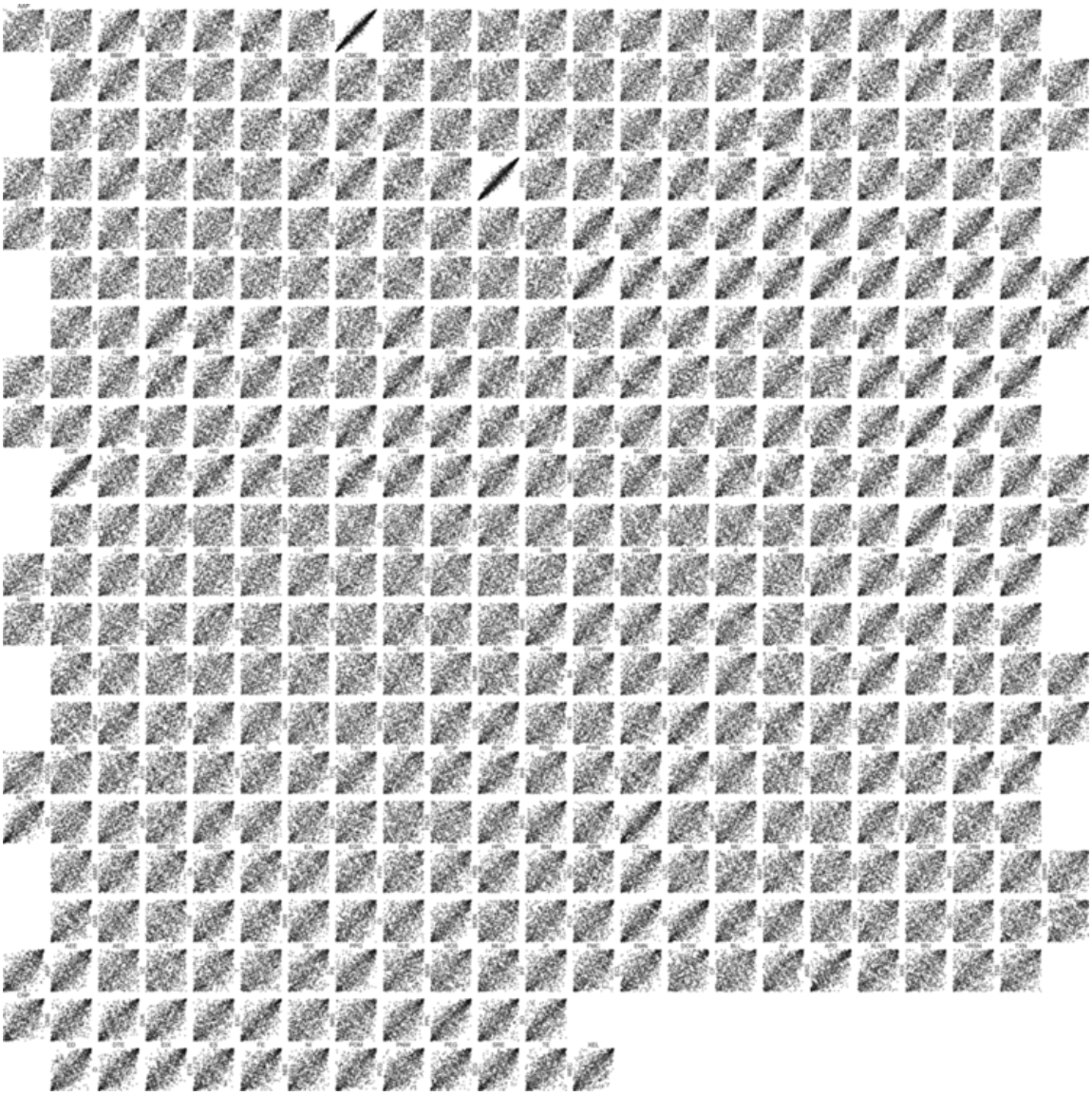

Figure 4 A zenplot of the pseudo-observations showing the pairs $(1,2),(2,3),\ldots,(d-1,d)$ for $d = 465$.

3.2 Zenpaths

Although a zenplot shows twice as many distinct pairs as does a scatterplot matrix in the same space, there are still a great many pairs that could be shown. For $d = 465$ dimensions there are $\binom{d}{2}$ =107,880 distinct plots. Of these, the zenplot of Figure 4 showed a little fewer than 500 or about 0.5% of all that are possible. To look at all plots would require more than 200 zenplots of the size of that shown in Figure 4 (or more than 400 scatterplot matrices); see also our comment in the last paragraph of Section 4.

Better would be to show only the *most interesting* pairs of plots. Here again the zenplot layout has an enormous advantage over the scatterplot matrix, simply by not being restricted to a matrix layout. Instead, the zenplot displays a particular path (or series of paths) through the scatterplot matrix.

To see this, imagine the $d \times d$ scatterplot matrix. A path can be followed through this matrix beginning at any plot and jumping to any other plot in the same row or column, thus sharing either a vertical or horizontal axis, and continuing in this fashion to produce a path of any desired length; see Hurley and Oldford (2011b). A *zenpath* is any such path which alternates between searching along a row and along a column (that is, a 3d transition path of Hurley and Oldford (2011b)).

A (default) zenplot display lays out the scatterplots in the order in which the variates appear in the dataset. Figure 4, for example, follows the variate order $1, \ldots, d$ which corresponds to the zenpath starting at the top left corner of the scatterplot matrix and zigzagging alternating right (same row) and downward (same column) crossing the variate name on the diagonal to the next plot each time. The path ends when the bottom right corner is reached. To follow any particular zenpath, then, the variate order in the dataset is simply changed to that of the desired zenpath before zenpath is called.

When a measure of interestingness can be assigned to each scatterplot, then we might restrict our displays to show only those plots of interest. These can be laid out as a zenpath (or series of disconnected zenpaths) following the graph theoretic methods of Hurley and Oldford (2010); Hurley and Oldford (2011b) and automated using the R package `PairViz` of Hurley and Oldford (2011a).

For financial data like the S&P 500, interest often lies in the dependence between the negative log-returns of any two stocks. Two common dependence measures for such data are Kendall's tau and Spearman's rho (both are measures of concordance in the sense of Scarsini (1984)) on the residuals. Or, as in certain quantitative risk management applications, we might be interested primarily in what happens in the extremes, that is in some measure of tail dependence between the two returns. In what follows, we focus on the latter case.

3.2.1 Tail dependence based on pairwise fitted t copulas

Here we choose to measure the (upper) tail dependence between each pair of negative log-returns by fitting bivariate copulas. To be concrete, for any (Z_1, Z_2) with joint distribution function H, continuous marginal distribution functions F_1, F_2, and corresponding marginal

quantile functions Q_1, Q_2, a measure of upper tail dependence, for any $p \in [0,1]$, can be taken to be $\mathbb{P}(Z_2 > Q_2(p) \,|\, Z_1 > Q_1(p))$. This probability is symmetric in Z_1 and Z_2 and the larger it is, the greater is the dependence between Z_1 and Z_2 in the top right corner of the bivariate distribution. Taking its limit as $p \to 1$, we have the *coefficient of upper tail dependence*

$$\lambda = \lim_{p \uparrow 1} \mathbb{P}(Z_2 > Q_2(p) \,|\, Z_1 > Q_1(p)).$$

This is often of interest when modelling joint high quantile exceedances in quantitative risk management. If the bivariate copula for H is C, then it is easy to show that

$$\lambda = \lim_{p \uparrow 1} \frac{1 - 2p + C(p,p)}{1-p} \tag{2}$$

and so the coefficient depends only on the underlying copula C of H and not on the margins F_1, F_2.

In higher dimensions practitioners have begun working with matrices $\Lambda = (\lambda_{ij})_{ij}$ of pairwise upper tail-dependence coefficients; see Embrechts et al. (2016) for a characterization and practical application.

Estimating λ directly from the data is difficult since there will be no pseudo-observations larger than p for any $p > \frac{T}{T+1}$. Instead, parametric copula models could be fitted to the pseudo-observations (1) of each pair of variables and the implied tail-dependence coefficients be computed (based on equation (2)) to construct a (pairwise) estimate of Λ.

To this end we will use bivariate t copulas and fit them using the approach of Mashal and Zeevi (2002) (see also Demarta and McNeil (2005)) as newly available in the R package `copula` via `fitCopula(, method = "itau.mpl")`; see Hofert et al. (2005). In terms of the fitted degrees of freedom ν and the correlation ρ (the off-diagonal element of the bivariate t copula's scale matrix P), the upper tail-dependence coefficient λ of a t copula is

$$\lambda = 2t_{\nu+1}\left(-\sqrt{\frac{(\nu+1)(1-\rho)}{1+\rho}}\right), \tag{3}$$

where $t_{\nu+1}(x)$ is the distribution function of the t distribution on $\nu+1$ degrees of freedom evaluated at x. Replacing the parameters by their estimates gives an estimate for λ.

Figure 5 shows pairwise estimated upper tail-dependence coefficients λ for all $\binom{d}{2} = 107,880$ pairs. At left, these are displayed in a matrix arrangement analogous to a scatterplot matrix except that, instead of a scatterplot, in each cell the value of the corresponding λ estimate is shown using a grey-scale encoding. This is essentially the pairwise estimated matrix Λ. At right, the overall density of all pairwise λ estimates is shown. Most values, for example, are less than 0.3.

The rows (columns) of the estimated matrix Λ are arranged in Figure 5 so that stocks in the same GICS sector, and within each sector in the same sub-sector, appear next to each other in the same row (column). The boundaries between sectors are marked by dashed

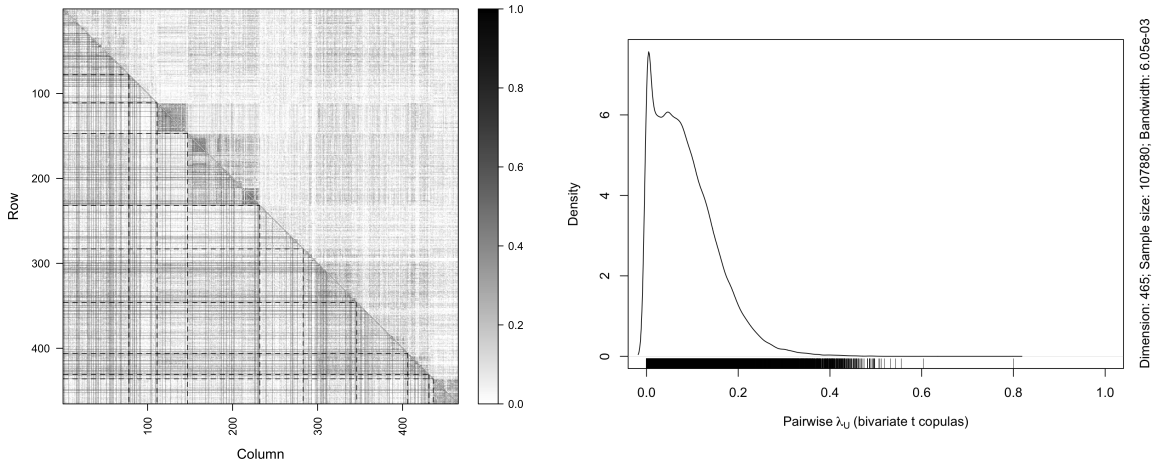

Figure 5 Pairwise estimated upper tail-dependence coefficients λ from fitted bivariate t copulas (different degrees of freedom). At left is the entire matrix Λ with GICS sectors (dashed lines) and sub-sectors (finer solid lines) indicated; at right is a plot of the estimated density of all $\binom{d}{2}$ pairwise entries of Λ.

lines appearing below the diagonal. The sectors appear top to bottom (left to right) in alphabetical order as before, namely: "Consumer discretionary" (78 constituents = first 78 rows), "Consumer staples" (33), "Energy" (36), "Financials" (85), "Health care" (51), "Industrials" (63), "Information technology" (60), "Materials" (25), "Telecommunications services" (5), and "Utilities" (29). Fine lines below the diagonal mark the sub-sectors within each sector (more easily discerned by zooming in on the display).

Even with such low estimated values for the upper tail-dependence coefficients, some structure is revealed by the estimated matrix Λ of Figure 5. The darkest blocks along the diagonal correspond to stocks in the same sector and within the same sub-sector. The third diagonal block down, for example, shows relatively stronger tail dependencies existing between constituents of the "Energy" sector. Such information can, for example, be used to set up a hierarchical dependence model with different within-sector dependencies than between-sector dependencies. Off the diagonal, the very light region immediately above the dark diagonal "Energy" block suggests overall little dependence between the constituents of the "Energy" sector and those of the "Consumer staples" sector. The cell values of Λ can thus help determine which corresponding scatterplots of pseudo-observations to examine more closely along some zenpath(s) of interest.

Finding interesting zenpaths from Λ has been automated by the function `zenpath()`. In Figure 6 `zenpath()` was used to find the ten pairs having largest upper tail dependence and the ten pairs having least upper tail dependence. All twenty plots are arranged in order from highest upper tail dependence to lowest upper tail dependence. The zigzag pattern is followed exactly as in Figure 4 except now there are occasional places showing only a couple

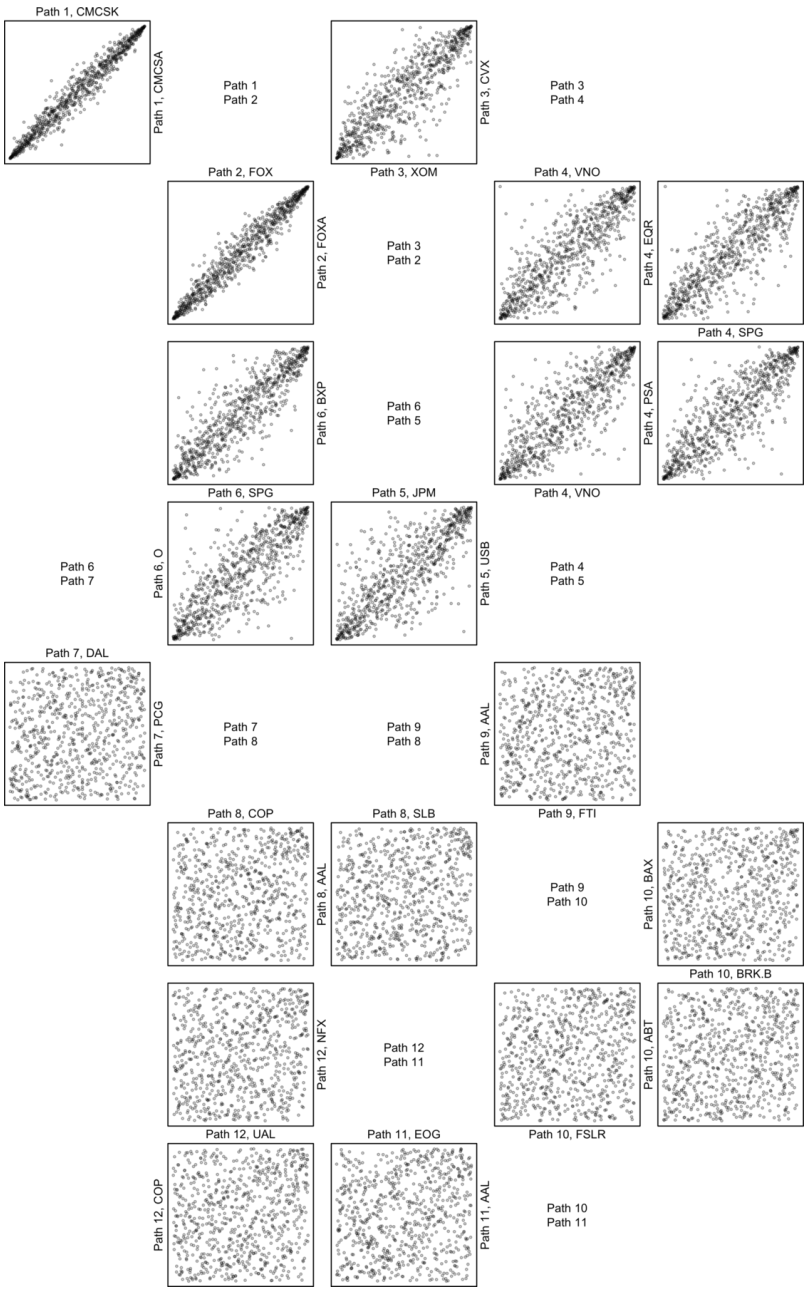

Figure 6 A zenplot constructed from a zenpath displaying the pseudo-observations of those 10 pairs of variables with largest (first) and then those 10 pairs with smallest (last) upper tail-dependence coefficient. When variables along the path are connected, they are displayed in one contiguous zenpath, abbreviated by Path 1–Path 12. Concatenated paths are separated by a block marking the transition from one path to another.

of labels where a scatterplot might have been expected. The reason for this is that these places mark boundaries where one zenpath ends and another one begins. Recall that a zenpath connects plots which share a variate (by alternating row and column selections in a scatterplot matrix). When no such variate is shared the zenpath ends and a new one begins (the change being equivalent to moving from one cell in a scatterplot matrix to another in a different row *and* different column). The zenplot of Figure 6 is the concatenation of twelve different zenpaths.

The two strongest upper tail-dependencies are those we have already seen, namely the two classes of Comcast shares and the two classes of Twenty-first Century Fox shares. Because these two pairs share no variates, they define the first two zenpaths (each of length one plot, or two variates) and are separated by the space labelling the end of path 1 and the beginning of path 2. The third path, also of length one, consists of the pair of stocks from the "Energy" sector, `CVX` (Chevron Corp.) and `XOM` (Exxon Mobil Corp.). Next is a path of length four, consisting of the variates `VNO` (Vornado Realty Trust), `EQR` (Equity Residential), `SPG` (Simon Property Group Inc), and `PSA` (Public Storage), all from the "Financials" sector. The stock `VNO` appears in two of these four pairs. Path 5 consists of the two "Financials" sector stocks `USB` (U.S. Bancorp) and `JPM` (JPMorgan Chase & Co.) and path 6 of three more, `BXP` (Boston Properties), `SPG` (Simon Property Group Inc), and `O` (Realty Income Corporation). Note that every pair of variates, of the ten having the strongest upper tail-dependence coefficient, is formed from stocks from the same GICS sector.

The variate pairs with weakest upper tail dependence appear in the bottom half of Figure 6 and are essentially indistinguishable from uniform scatterplots (see Figure 2(a)). This suggests that the standardized residuals of these pairs can be considered independent. There are again six paths: path 7 `DAL` (Delta Air Lines) from the "Industrials" sector, `PCG` (PG&E Corp.) from the "Utilities", path 8 `COP` (ConocoPhillips) "Energy", `AAL` (American Airlines Group) "Industrials", and `SLB` (Schlumberger Ltd.) "Energy", path 9 `AAL` (American Airlines Group) "Industrials", and `FTI` (FMC Technologies Inc.) "Energy", path 10 `BAX` (Baxter International Inc.) "Health Care", `BRK.B` (Berkshire Hathaway) "Financials", `ABT` (Abbott Laboratories) "Health Care", and `FSLR` (First Solar Inc) "Information Technology", path 11 `AAL` (American Airlines Group) "Industrials", and `EOG` (EOG Resources) "Energy", and finally path 12 `NFX` (Newfield Exploration Co) "Energy", `UAL` (United Continental Holdings) "Industrials", and `COP` (ConocoPhillips) "Energy". Note that the ten pairs of variates with weakest upper tail dependence are from different GICS sectors.

Given that the weakest dependencies occur between constituents from different GICS sectors, one might ask what pairs of constituents from different sectors have the strongest upper tail dependencies. To answer this, Figure 7 shows the ten such cross sector pairs having greatest tail dependence in descending dependence order. An examination of the individual constituents reveals that every pair has one stock from the "Industrials" sector most frequently paired with either a "Materials" one (5 pairs), or with an "Information Technology" stock (3 pairs). Furthermore, in all ten pairings an examination of the companies suggests that the dependence is not really surprising – for example, the strongest is between

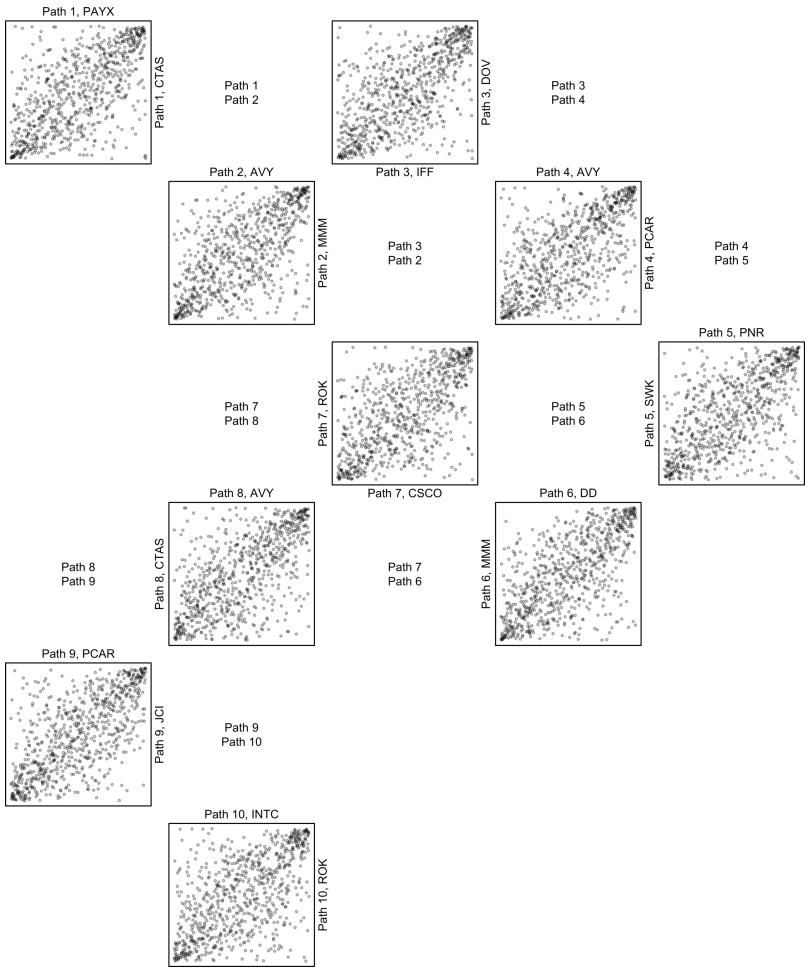

Figure 7 A zenplot constructed from a zenpath displaying the pseudo-observations of those 10 pairs of variables with largest upper tail-dependence coefficient which belong to different GICS business sectors.

PAYX a provider of human resource outsource services from the "Information technology" sector and CTAS from the "Industrials" sector that provides such "diversified support services" as corporate identity, promotional services, restroom cleaning, and supplies, and the weakest dependence of the ten is between Intel Corp. (INTC, "Information Technology") and Rockwell Automation Inc. (ROK, "Industrials").

Note that there are as many paths in Figure 7 as there are pairs displayed. Although some constituents appear more than once (for example, AVY Avery Dennison Corp. (3), CTAS Cintas Corporation (2), MMM 3M Company (2), PCAR PACCAR Inc. (2), and ROK Rockwell Automation Inc. (2)), nowhere along the zenpath of decreasing upper tail dependence is one of the repeated constituents shared by consecutive plots.

Similarly, recall that in Figure 6 the ten strongest dependencies corresponded to pairings of constituents from the *same* GICS sector. Unfortunately, the ten strongest pairings came only from three different sectors: "Consumer discretionary", "Energy", and "Financials". This misses seven out of the ten GICS sectors. We might ask, then, what pair of constituents within each and every sector has the largest upper tail dependence?

Figure 8 shows a zenplot of the ten GICS sectors (in alphabetical order as before) as ten separate zenpaths labelled GICS 1–GICS 10. Within each sector, the constituent pairs are sorted from greatest to least dependence.

The first plot in the path of each sector in Figure 8 displays the pseudo-observations for that pair of constituents having the largest upper tail-dependence coefficient within that sector. For each sector, the zenpath beginning at that pair continues in decreasing tail dependence as long as the path is connected; it ends as soon as the path ends in that sector. For example, within the first GICS sector ("Consumer discretionary") only one pair appears, as no connection to the next pair within that sector can be made according to the zenpath of decreasing tail dependence; this is why the strong relation between the FOX and FOXA shares of Figure 6 do not also appear in Figure 8. However, the second sector ("Consumer staples") the two pairs with strongest tail dependence share the variate PG (Procter & Gamble) and so appear as a connected pair joining three well known companies (from two different sub-sectors) offering personal and household products (viz. KMB (Kimberly-Clark), PG, and CL (Colgate-Palmolive)).

The concatenated zenpaths of Figure 8 separate the groups visually and give some sense of their size. The groups, their stocks in order, and the sub-sectors to which they belong are as follows: GICS 1 or "Consumer discretionary" (CMCSK and CMCSA, both Comcast); GICS 2 or "Consumer staples" (KMB (Kimberly-Clark), PG (Proctor & Gamble), and CL (Colgate-Palmolive) from two closely related but different personal or household product sub-sectors); GICS 3 or "Energy" (XOM (Exxon), CVX (Chevron), COP (ConocoPhillip), from two closely related but different oil & gas sub-sectors); GICS 4 or "Financials" (VNO (Voronado), EQR (Equity residential), SPG (Simon Property group), PSA (Public Storage), and VNO again, all "REITs"); GICS 5 or "Health care" (ANTM (Anthem Inc.), AET (Aetna), CI (CIGNA Corp.) , and ANTM again, all "Managed health care"); GICS 6 or "Industrials" (NSC (Norfolk Southern), UNP (Union Pacific), CSX (CSX Corp.), all "Railroads"); GICS 7 or "Information technology" (XLNX (Xilinx Inc.), ALTR (Altera Corp.), both "Semiconductors");

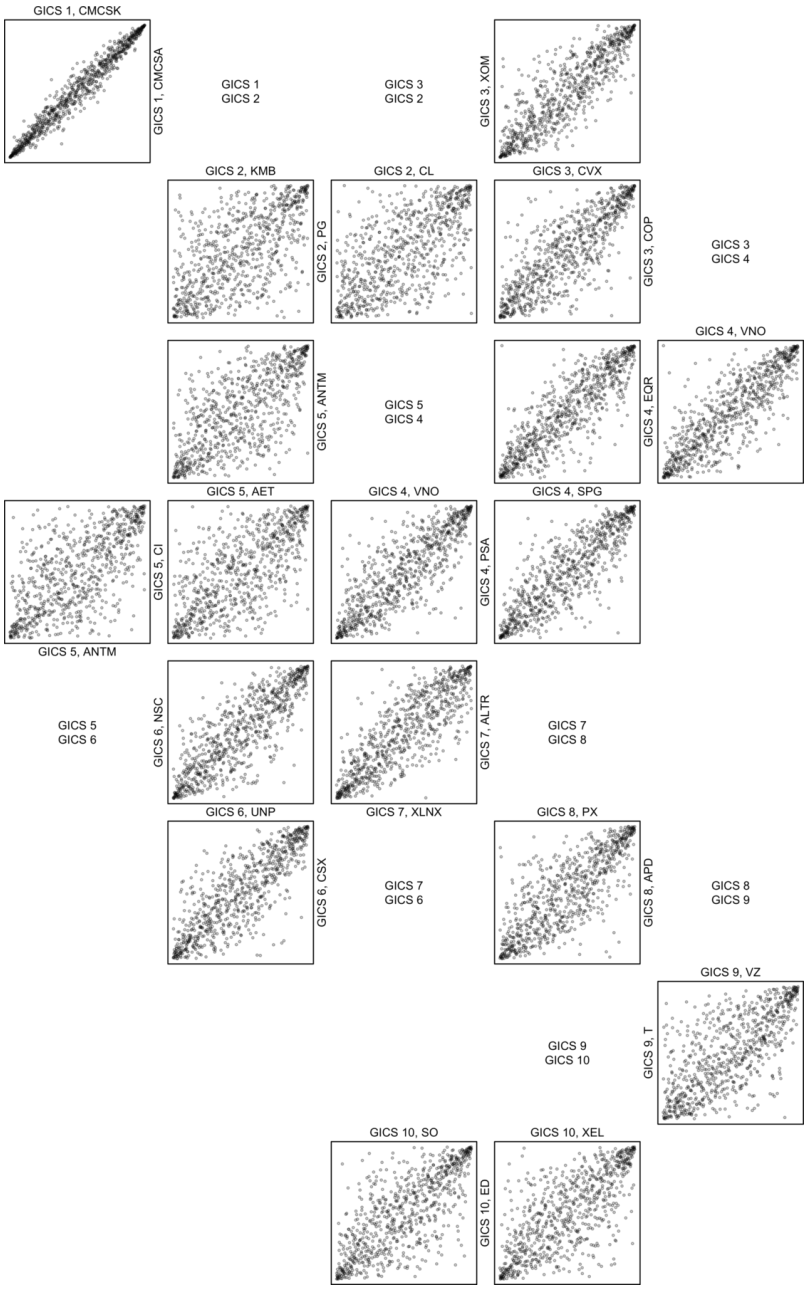

Figure 8 A zenplot constructed from a zenpath displaying the pseudo-observations of those groups of connected pairs of constituents with largest upper tail-dependence coefficient within each GICS business sector; the latter (in alphabetical order) are labelled GICS 1–GICS 10.

GICS 8 or "Materials" (PX (Praxair), APD (Air products and chemicals), both "Industrial gases"); GICS 9 or "Telecommunication services" (VZ (Verizon), T (AT&T), both "Integrated telecom services"); and GICS 10 "Utilities" (XEL (Xcel Energy Inc.), ED (Consolidated Edison), SO (Southern Co.), two "Electric utilities" one "MultiUtilities"). The zenplot has clearly picked out some interesting related groupings with many of the strongest relations within a sector also appearing within the same (or closely related by definition) sub-sector.

Clearly some sectors show much weaker within-sector dependence than do others. We could continue in this way, using zenplots to more deeply explore dependence within or between sectors and sub-sectors. Instead, we now turn our attention to how zenplots might also be used in assessing the models we are using.

4 Model assessment

Zenplots can be used to quickly arrange nearly any visual display in a compact but informative way. Here we illustrate how zenplots, as well as some other displays, might be used in the very important task of model assessment.

4.1 Checking marginal distributions

We modelled each component series of negative log-returns by an ARMA$(1,1)-$GARCH$(1,1)$ model with t innovations. The latter model assumption can be assessed visually via a quantile-quantile plot (or Q-Q plot) of the sample quantiles of the observed returns.

Figure 9 shows Q-Q plots for sixteen components. The vertical axis of each Q-Q plot marks the sample quantiles and the horizontal axis marks the theoretical quantiles for a standardized t distribution with degrees of freedom estimated from the sample. The estimated degrees of freedom, $\widehat{\nu}$, is shown in each plot below the ticker symbol for that return. The grey regions are point-wise empirical confidence envelopes for each quantile as constructed from 1,000 samples (each of size $n = 755$) generated from a t marginal on the estimated degrees of freedom. From darkest to lightest, the regions correspond to the central 90, 95, and 99% of the simulated sample quantiles as well as the range of all 1,000 generated. Departures from the marginal $t_{\widehat{\nu}}$ hypothesis are seen as points appearing at the extremities (or outside) of the given grey regions; see Oldford (2016) for details.

The sixteen components chosen were those that showed the greatest evidence (as determined by an Anderson–Darling test) against the hypothesis that the marginal ARMA$(1,1)-$GARCH$(1,1)$ residuals follow a standardized $t_{\widehat{\nu}}$ distribution. The test's observed significance level (SL) is given on each plot and the plots are displayed following a zenpath in order of increasing observed significance levels (that is, decreasing evidence against the hypothesis).

The first three stocks TEL (TE Connectivity Ltd.), DFS (Discover Financial Services), and DAL (Delta Air Lines) each have an extraordinarily small significance level (or p-value) of SL < 0.0001 which in turn means extraordinarily strong evidence against the hypothesis. Similarly strong evidence is given visually by their Q-Q plots showing massive outliers.

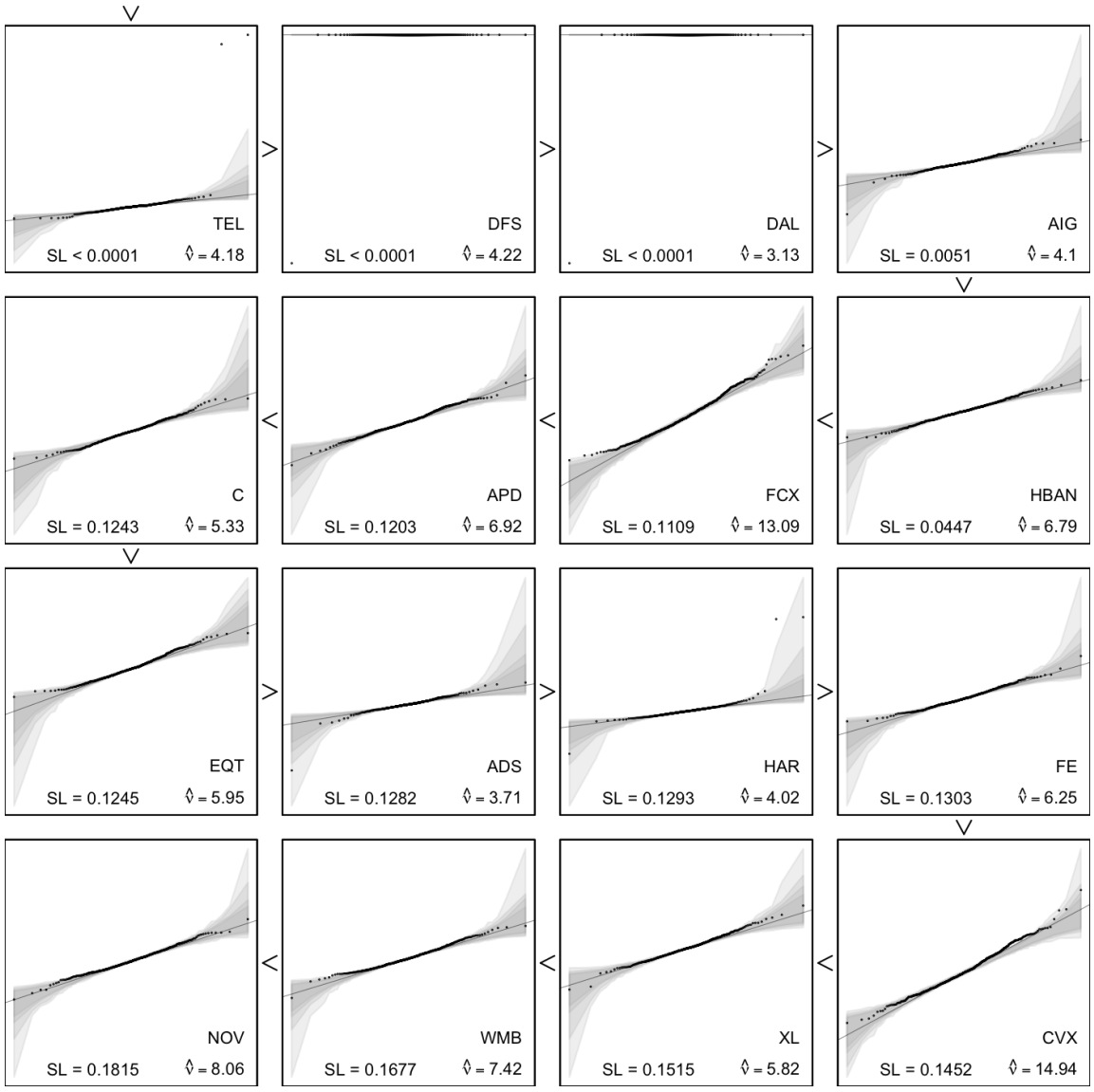

Figure 9 A zenplot of Q-Q plots for those 16 margins having the most significant Anderson–Darling test statistics; observed significance levels (SL) and the fitted degrees of freedom ($\widehat{\nu}$) are as indicated at the bottom of each plot. The line of exact agreement (the $y = x$ line) appears as a fine line in each plot. For the margins `TEL`, `DFS`, `DAL`, and `AIG` the Anderson–Darling test leads to strong evidence against hypothesis; the Q-Q plots identify more.

This is perhaps not too surprising since these three stocks are exactly those having large numbers of missing values as shown in the right hand plot of Figure 1. The missing values appear at the beginning and were replaced in each by a single value – it would be more surprising had the implied standardized residuals actually followed a $t_{\widehat{\nu}}$ distribution.

Similarly, it should be no surprise that `AIG` (American International Group) shows up next in order as not having a t innovation distribution. During the subprime mortgage crisis of 2008 AIG stock collapsed and would have failed entirely had it not been bailed out. This is picked up numerically by an Anderson–Darling test (SL ≈ 0.0005) and visually by the Q-Q plot as several of the positive standardized residuals are outside the range of the simulated envelopes on the right where the envelope is tight, just before it fans out.

The Anderson–Darling test for `HBAN` (Huntington Bancshares) is less compelling (SL $= 0.0447$) but still provides some evidence against the hypothesis of a standardized $t_{\widehat{\nu}}$ residual margin. In contrast, the Q-Q plot for `HBAN` provides no evidence whatsoever against the hypothesis.

Conversely, the Anderson–Darling test finds no evidence against the $t_{\widehat{\nu}}$ hypothesis for any remaining whereas several Q-Q plots clearly show evidence to the contrary: for example, `HAR` (Harman International Industries, Inc.) and `ADS` (Alliance Data Systems, Inc.) with outlying residuals, and `FCX` (Freeport-McMoRan), `C` (Citigroup, Inc.), `EQT` (EQT Corp.), `CVX` (Chevron Corporation), and `WMB` (Williams Companies, Inc.) all showing asymmetry.

Graphical methods are able to detect many different types of departures and, with zenplots it actually becomes feasible to view 465 Q-Q plots.

4.1.1 More general zenplot layout

Some important features of zenplot construction enabled the compact layout of Q-Q plots as in Figure 9 and make practical viewing of all 465 plots possible.

First, a zenplot is actually a layout of an alternating sequence of single coordinate and two-coordinate plots; in Figure 9 the alternation is between a "V" arrow shape (one dimensional location indicating an order) and a Q-Q plot (having two coordinates to be plotted).

Second, the location of each plot is determined by where it appears in a sequence of "direction" indicators, one of "u", "d", "l", or "r", for "up", "down", "left" or "right"; each one is the directive for where the *next* plot will appear relative to the present plot. The plots of Figure 9 begin as the top left "V" drawn to indicate "d" for the relative position of the first Q-Q plot. It then follows a series of eight "r" directions to move across the page alternating Q-Q plots and arrows, then two "d" to place the arrow down and to position the following Q-Q plot down on the next row. This Q-Q plot exits left (direction "l") to start the sequence moving leftward back across the page. The zenplot thus zigzags back and forth across the page moving down when the edge of the page is reached and then reversing the horizontal direction. The zenplots of all previous figures were constructed using a slightly more complex sequence of directions; see the demo `SP500` for the corresponding source code. By using an appropriate sequence of directions, essentially any layout pattern of

alternating plots can be constructed with a zenplot (for example, a spiral; see `?zenplot` for more details and additional features not described here).

Third, there is no restriction on the plots that may be drawn. The Q-Q plot used in Figure 9, for example, is not from the `zenplots` package of Hofert and Oldford (2016) but from `qqtest` of Oldford (2014). If a plot can drawn in any one of three R plotting systems of `graphics`, `grid`, or `loon`, it can be part of a zenplot.

4.2 Modelling via a full t copula

The approach taken so far is very flexible, in that it allows separate t copula models for every pair of variates (an even more flexible nonparametric approach is sketched in Appendix A.1). This is possible as we are here, exemplarily, only interested in the notion of bivariate tail dependence; this, of course, does not guarantee the existence of a valid model in 465 dimensions. If the latter is required, a more standard approach is to fit a joint copula model for all 465 variates at once. An obvious candidate is the multivariate t copula since it has been known to fit multivariate financial return data comparably well and it *can* be fit to such a large number of dimensions using the fitting procedure of Mashal and Zeevi (2002); the latter was newly implemented in the R package `copula` for this purpose.

4.2.1 Tail dependence

As with the pairwise modelling, this fully joint model will have correlation parameters from whose estimates, via Equation (3), an estimate of the upper tail dependence for any pair of returns can be obtained. These measures from the full model can then be examined as before.

Figure 10, is the equivalent of Figure 5, except now the $\widehat{\lambda}$s have been estimated from the *full* 465-dimensional, t copula model. The matrix display at left is similar in pattern to its counterpart from Figure 5. The most dramatic difference between the two is that the matrix of Figure 10 looks like a washed out version of that of Figure 5, that is, the full model suggests weaker pairwise upper tail dependencies than do the separate pairwise models. Comparing the two densities of the two sets of estimates from the right hand displays of Figures 10 and 5, we see that the full model has reduced the range of the bulk of the dependence estimates from less than 0.3, to less than 0.1.

Matching corresponding estimates of λ from the two models, we can compare their values more directly. Figure 11(a) displays the density of their differences showing that the estimates from the separate pairwise models are typically larger (often by more than 0.1) than those from the joint model. Figure 11(b) plots these estimates as pairs; the points lying below the $y = x$ line are cases where separate pairwise modelling estimates larger upper tail dependencies than does the joint copula model. Dependence between the two sets of upper tail-dependence coefficient estimates is summarized by the pseudo-observations from the upper tail-dependence coefficients plotted in Figure 11(c) which suggest an asymmetric dependence.

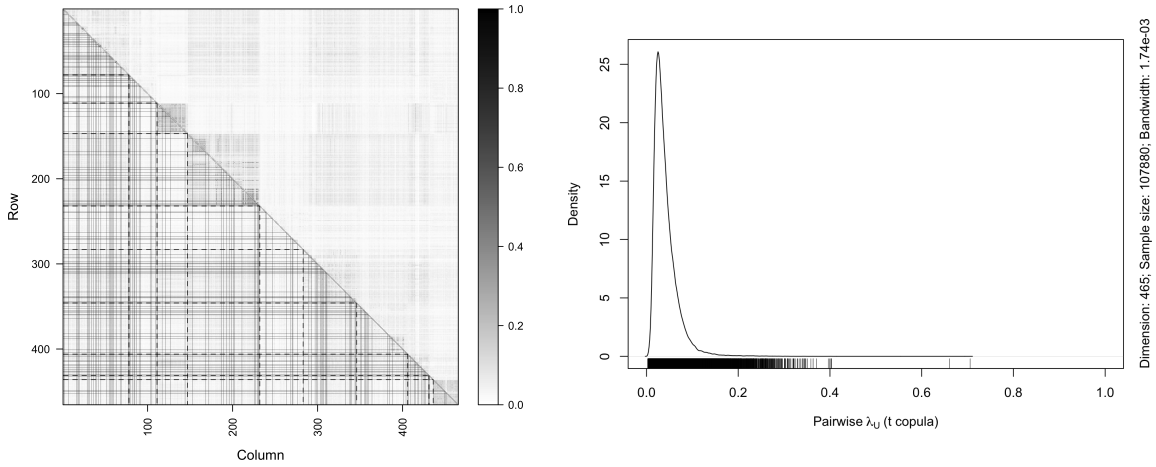

Figure 10 Matrix of implied upper tail-dependence coefficients as obtained from a fitted joint t copula (left-hand side); the fitted degrees of freedom were 12.98. Density plot of the corresponding $\binom{d}{2}$ entries (right-hand side).

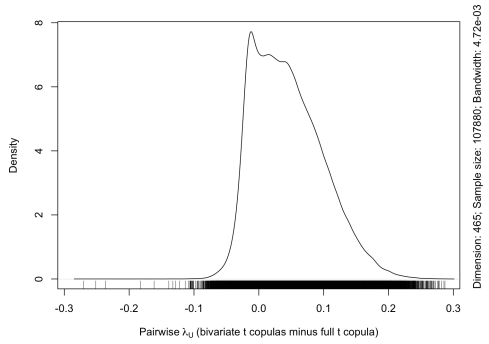

(a) Differences between $\widehat{\lambda}$.

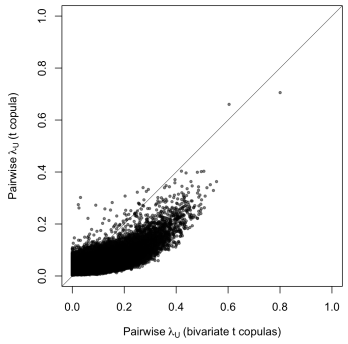

(b) Coefficients $\widehat{\lambda}$.

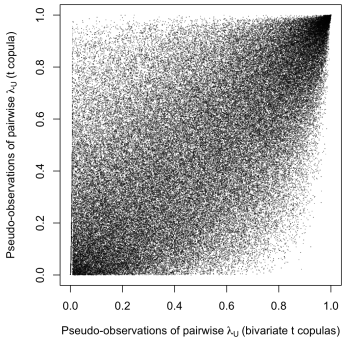

(c) Pseudo-observations of the λs.

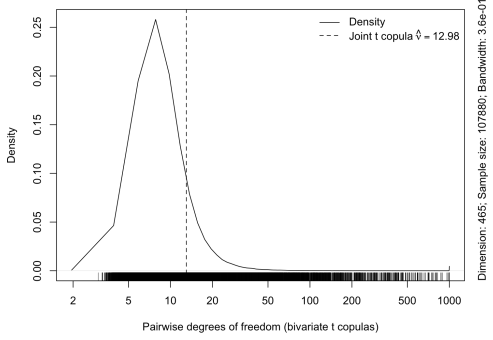
Density
Joint t copula $\hat{\nu}$ = 12.98
Density
Pairwise degrees of freedom (bivariate t copulas)
Dimension: 465; Sample size: 107880; Bandwidth: 3.6e-01

(d) Degrees of freedom.

Figure 11 Comparing estimates: joint t copula and the separate pairwise t copula models.

Note that the joint t copula has only a single degree of freedom parameter, shared by all pairs, whereas the separate pairwise models have a potentially different degrees of freedom value for every pair. The density of the degrees of freedom from the pairwise models is shown in the right-hand plot of Figure 11; the single estimated degrees of freedom of the full t copula, 12.98, is shown as the vertical line. As can be seen, the pairwise models suggest heavier tails (lower degrees of freedom) in general than does the joint model. The dramatic restriction on the degrees of freedom forced by the full model seems to force lighter tails on most of these pairwise t copulas.

4.2.2 Overall goodness of fit

We already have seen some evidence against the hypothesis that the joint model has a multivariate t copula. In Section 4.1, for example, there was evidence against a t distribution for the estimated standardized residuals for some marginal negative log-returns. And in Figure 11, the differences seen between the full model and the more flexible separate pairwise models also suggest evidence against the full model (for example, when not constrained to be identical, the degrees of freedom from the pairwise fits were highly variable and lower than that estimated by the full model).

For an overall goodness of fit test, getting approximate significance levels from a parametric bootstrap based on the Cramér–von Mises functional S_n as in Genest et al. (2009, Eq. (2)) would be a general approach particularly for few dimensions. In the present case, however, we have $d = 465$, and the approach involves evaluating multivariate t distribution functions on non-integer degrees of freedom which is currently not available in R. Furthermore, we need to compute tests for all fitted pairwise t copulas – all of which will need to be repeated as many times as we have bootstrap replicates to produce approximate significance levels. Even with such efficient fitting procedures as that of Mashal and Zeevi (2002), the computational burden is prohibitive for our present purposes, namely the illustration of model checking and of zenplots in this context.

Instead, we construct a goodness of fit test for the full model based on an Anderson–Darling test of observations derived from (a function of) the Rosenblatt transformations of the pseudo-observations. While not as general, this method has the advantage that the same derived observations can also have their distribution assessed visually using a self-calibrating Q-Q plot.

The derived observations will be constructed as follows. For a random vector $\boldsymbol{U} \sim C$ for some copula C, we can transform $\boldsymbol{U} = (U_1, \dots, U_d)$ to $\boldsymbol{V}$ as

$$\begin{aligned} V_1 &= U_1, \\ V_2 &= C_{2|1}(U_2 \,|\, U_1), \\ &\vdots \\ V_d &= C_{d|1,\dots,d-1}(U_d \,|\, U_1, \dots, U_{d-1}), \end{aligned}$$

where $C_{j|1,\dots,j-1}$ denotes the conditional copula of U_j given $U_1, \dots, U_{j-1}$, $j \in \{2, \dots, d\}$. This embeds the conjectured copula in the calculations and, following Rosenblatt (1952), the transformed random vector $\boldsymbol{V}$ will follow a $\mathrm{U}(0,1)^d$ if and only if the copula C is correct (that is, the true underlying copula). Note also that this construction depends on the order of the variates in the Rosenblatt transformation.

The realization $\boldsymbol{v}$ of the variate vector $\boldsymbol{V}$ is determined using the `cCopula()` function from the R package `copula`. Since the calculations can numerically produce many tied values at 0 and at 1 for the v_js, the v_js actually used will be the pseudo-observations of the Rosenblatt calculated v_js. The corresponding random vectors of the pseudo-observations will also be uniformly and independently distributed within the d-dimensional unit hypercube if C is correct.

Any mapping $g : [0,1]^d \to \mathbb{R}$ will produce a random variable $W = g(\boldsymbol{V})$ whose distribution, if known, may be tested via a numerical test like the Anderson–Darling or via a visual test like the self-calibrating Q-Q plot. Evidence against this distribution for W will provide evidence against the hypothesis that the copula C is correct.

For illustrative purposes, we choose $W = \sum_{j=1}^{d} \left(\Phi^{-1}(V_j)\right)^2$ where Φ is the standard normal distribution function. Now $W \sim \chi^2_d$ which may be assessed, either numerically or visually, on the realizations $w_1, \dots, w_T$.

For a numerical assessment, we apply an Anderson–Darling test to the putative χ^2_d realizations (as suggested by Breymann et al. (2003) for $d = 2^5$). The resulting significance level was on the order of 10^{-6} which is very extraordinarily strong evidence against the joint t copula on d dimensions.

For a visual test, Figure 12 shows Q-Q plots using two different orders of the Rosenblatt transformation. Note that for plotting purposes, these Q-Q plots first transform the realizations $w_1, \dots, w_T$ to $\sqrt{w_1/d}, \dots, \sqrt{w_T/d}$. The latter are realizations of the random variate $\sqrt{W/d} \sim K_d$ where $K_d = \sqrt{\chi^2_d/d}$ is the "kay" distribution on d degrees of freedom. The K_d is more nearly symmetric and concentrates around 1 as $d \to \infty$, giving more easily interpreted Q-Q plots than would the equivalent χ^2_d; see Oldford (2016). In assessing the fit visually, it is the shape of the curve of points as well as the number of points appearing near the edges of the envelopes. The curve should be very nearly a straight line for this many observations (particularly in the centre) but instead shows curvature about the centre – moving from one side of the envelopes in the centre to the opposite side in the tails. This may be more easily observed in Figure 12(b). The curvature indicates a poor fit to the K_{465} distribution from the asymmetry of the empirical distribution. Evidence against K_{465} implies evidence against the joint t copula model. It does not, however, appear as strong as that stated by the Anderson-Darling test (about 8×10^{-7} for the samples in each of Figures 12(a) and (b).

All evidence seems to point against the full t copula model.

[5] The limitations of this tests are known well; see, for example, Dobrić and Schmid (2007).

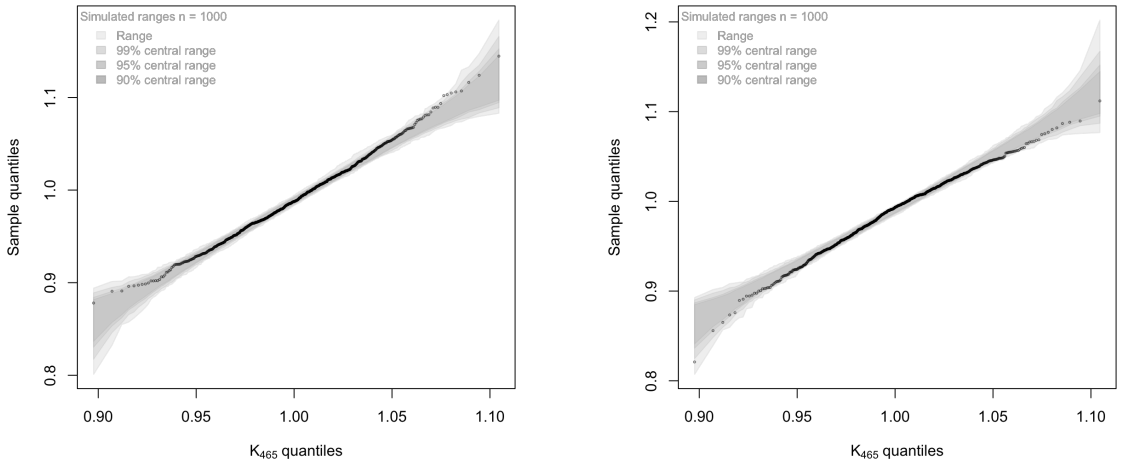

(a) in order $1, \ldots, 465$ (b) in randomly generated order

Figure 12 K_{465}-transformed Rosenblatt transformed pseudo-observations of the fitted full t copula.

4.2.3 Degrees of freedom? Or t at all?

The goodness of fit tests in the previous section may give evidence against the full t copula model for the joint innovation distribution of the marginal $\mathrm{ARMA}(1,1) - \mathrm{GARCH}(1,1)$ models of the negative log-returns, but they provide little information on *how* or *where* the full t copula fails to fit the observed data. To gain further insight, we test the bivariate marginal fits implied by the fitted full t copula following the same methodology as when testing the full model. Comparing these to the tests done earlier on the separate pairwise t copula models will shed light on whether to associate any pairwise lack of fit of the full model with its common degrees of freedom across all pairs, or with the t family itself whatever the degrees of freedom.

Figure 13(a) presents the matrices marking as points those pairs of returns having $\mathrm{SL} < 0.05$ from the Anderson–Darling test of these pairs as fit by the full t copula model. Stocks are ordered as before by sector and by subsector as marked below the diagonal. As the points are somewhat difficult to see (without zooming on the electronic copy), only those stocks appearing in any pair with $\mathrm{SL} < 0.05$ (together with diminished sectoral lines) are presented in Figure 13(b) where the lines identifying sectors have been.

The vast majority of cells (107,531 of 107,880 or $\approx 99.67649\%$) are empty, indicating little evidence ($\mathrm{SL} > 0.05$) against either the full t copula model with common degrees of freedom *or* the separate pairwise t model for that pair of returns. These pairs do not seem to be causing the overall lack of fit for the full model.

Coloured cells mark those pairs where testing the fitted t model for *both* the full and the pairwise models produced $\mathrm{SL} < 0.05$. There are 336 points in the matrix, representing 168 pairs of returns, for which neither (bivariate) t copula fits. These pairs suggest that the

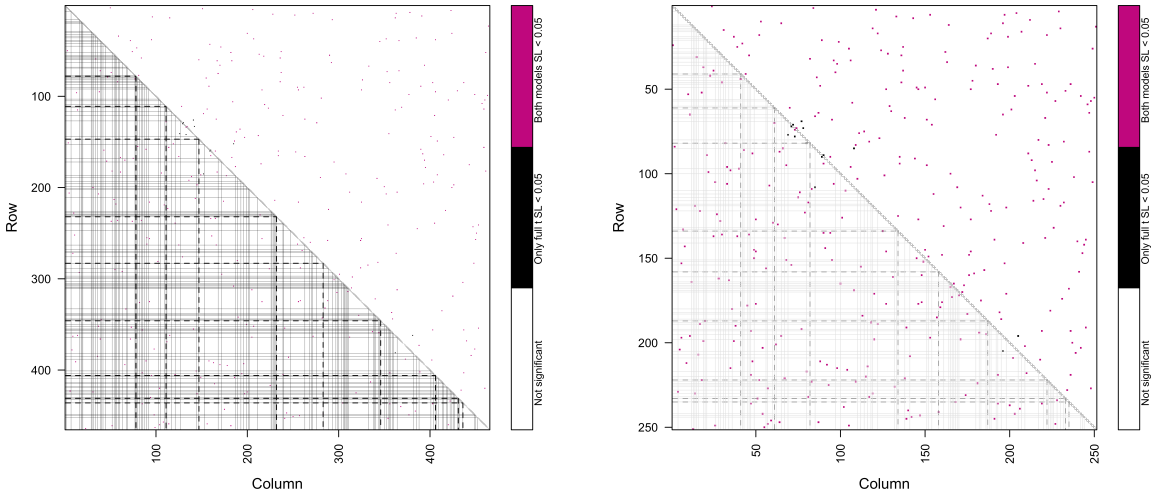

(a) All stock returns.

(b) Those having SL < 0.05 in at least one pairing.

Figure 13 Pairs of returns having significance level SL < 0.05 using an Anderson–Darling test from the fitted full t copula model. Points are coloured whenever SL < 0.05 also held for the separate pairwise fit (336 pairs) otherwise they are black (13 pairs).

choice of the t family is the problem, not the common degrees of freedom assumed by the full model.

Another 13 cells are shown as black, nearly all of which are near the diagonal of Figures 13(a) or (b). The points represent 7 pairs of returns for which SL < 0.05 when testing the full model but SL > 0.05 for the pairwise model. This suggests that for these innovations a t copula seems to fit but not one with the degrees of freedom from the full model fit. Instead, degrees of freedom here were in the 3–7 range as opposed to 13 for the full model. The stocks of each pair were invariably from the same sector and often from the same sub-sector (hence appearing near the diagonal of Figure 13(a).

There were 13 rather than 14 cells because one pair of returns (`WMB`, `VL`) had SL < 0.05 for one order of the pair (below the diagonal) in the Rosenblatt transformation and SL > 0.05 for the other order (actual values were ≈ 0.048 and 0.052 for which there is no scientific difference and which illustrate the well-known absurdity of using a hard and fast critical value as a cut-off in testing as opposed to reporting the actual significance levels observed). Significance levels from the remaining 6 pairs ranged from about 0.032 to 0.047.

Note that these tests are used here primarily to identify some pairs of returns which show greatest departure from the two assumptions: same degrees of freedom if t, and whether a t fits well or not. Using them collectively to test the model is also a bit problematic. The tests are not, for example, independent; had they been independent, and had the full model held, we would expect to see more than $5,000$ coloured cells in the matrix plot of Figure 13(a) and not so few as 349. Appendix A.2 explores this a little further, showing

the interesting dependence structure between the tests of the full model and those of the pairwise model.

Instead, we use these significance levels only to direct the analyst to those pairs of standardized residuals whose dependence structure might be more closely examined, namely those which are least consistent with a t copula model as measured by this Anderson–Darling test. Figure 14 lays out the pseudo-observations of these pairs of standardized residuals (every SL $< 3 \times 10^{-6}$); whenever adjacent plots share variates they are displayed in the same group (as determined by `connect_pairs(, duplicate.rm = TRUE)`). The pseudo-observations may now be critically examined by an experienced analyst to determine how each pair of standardized residuals appears to depart from a t copula and to possibly even suggest an alternative copula family[6].

A visual inspection can reveal departures other than those identified by the test statistic used to select the plot. For example, Anderson–Darling emphasizes departures in the hypothesized distribution's tails. The hypothesized distribution here, however, is χ^2_2 (albeit derived from a hypothesized t copula). The right tail of this χ^2_2 is constructed from large *and* small pseudo-observations and so does not necessarily identify a difference between the upper-right and lower-left of the plots of pseudo-observations. Rather, these two tails of the bivariate t copula are treated together, as one, in the assessment. Even so, examination of the plots of Figure 14 does reveal several showing an apparent asymmetry between the two densest corners, a well-known stylized fact of financial data not captured by a t copula. Asymmetry in the other direction can also be detected visually in several plots.

Similarly, the left tail of this χ^2_2 is constructed from pseudo-observations near 1/2 and so this Anderson–Darling test will emphasize differences from the centre of a t copula. Unusual spaces and/or densities in the centre of the plots might therefore be detected by this test. Indeed, the last plot (bottom-leftmost plot) of Figure 14 shows an extremely unusual central configuration. The returns involved are those of `DAL` and `DFS` which were also previously identified by the Q-Q plots of Figure 9. These were two of the three stocks that were missing many measurements early in the time period under study. This would seem to corroborate the value of the Anderson–Darling test on the middle part of the copula. Unfortunately, when the third incomplete stock, `TEL`, is plotted against either of `DAL` or `DFS`, the pseudo-observations also reveal strong linear (non t copula) patterns at the centre. Yet, neither plot is detected by Anderson–Darling.

Another problem with our use of the Anderson–Darling test revealed is numerical. Of the plots of Figure 14, all but the last one (that of `DAL` and `DFS`) have the same calculated significance level. This is because the squared normal probability integral transform for some of the putative uniforms actually returned `Inf` in R. This may not be such a problem for purposes of identifying pairs that are not t copulas, but it severely diminishes the utility of an ordered layout provided by zenplot. The first 167 plots of Figure 14 are unordered

[6] Note that this is not an easy task as replacing a bivariate model by another one can (and most often will) not lead to a proper multivariate model anymore; see also later. However, the information *how* the data departs from the hypothesized model is valuable in making a decision whether the latter is still acceptable for the modeling task at hand.

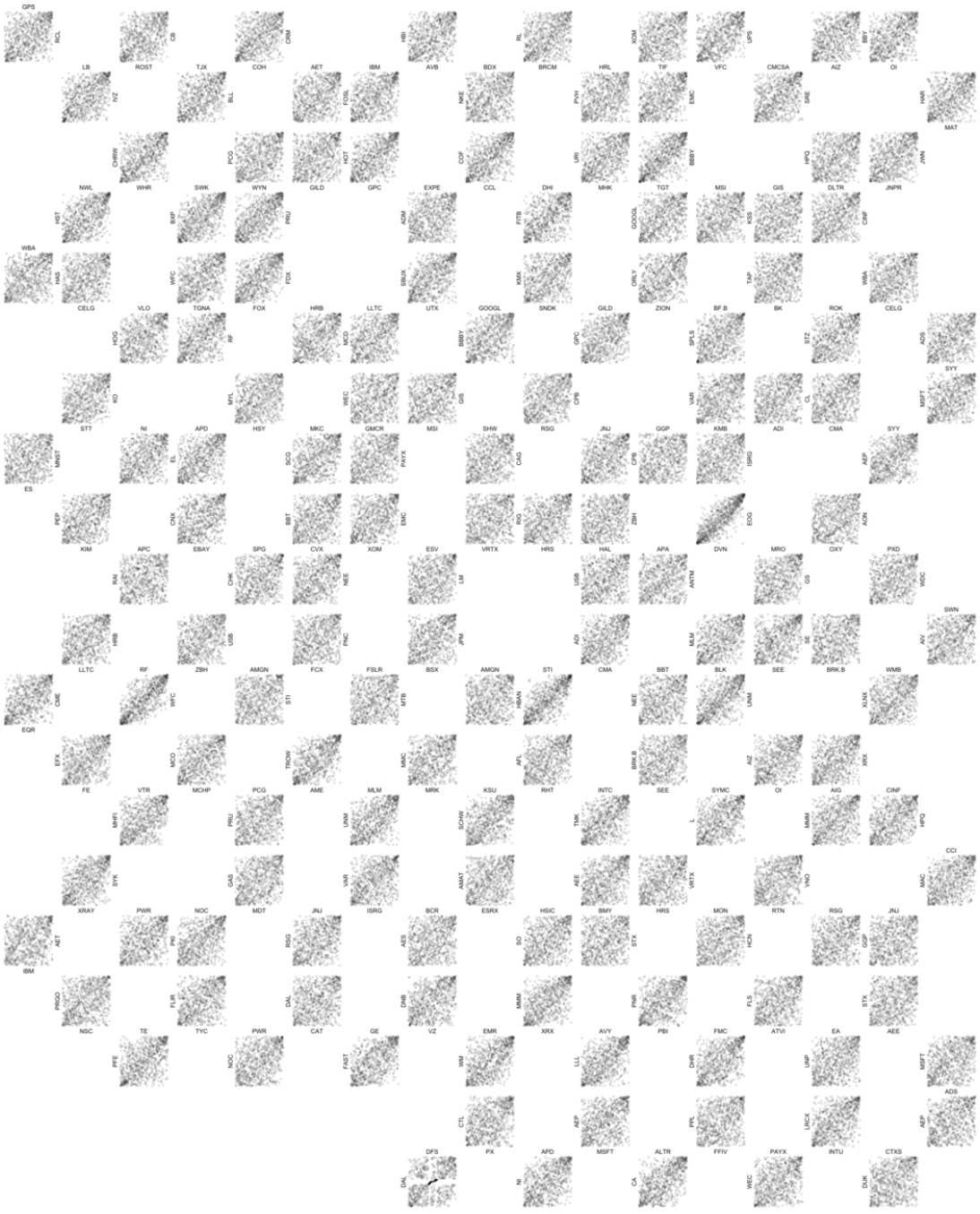

Figure 14 A zenplot constructed from a zenpath displaying the pseudo-observations of those pairs of variables having SL < 0.05 for both the full t copula and the bivariate t copula (based on the Anderson-Darling test); note that SL $< 3 \times 10^{-6}$ for all plots. The last plot has the largest significance level; remaining plots are in arbitrary order due to `qnorm(...)=Inf` occurring in these cases.

with respect to one another (though they do properly precede the last one).

Other criticisms can and have been levelled at the Anderson–Darling test and, as noted earlier, it would be better (and actually necessary) were it replaced by a parametric bootstrap; see Dobrić and Schmid (2007) and Genest et al. (2009)). As mentioned before, besides the challenge of determining arbitrary values of the cumulative distribution function of a multivariate t, with non-integer degrees of freedom, the computational burden alone of a parametric bootstrap for all pairs of such high-dimensional data is presently prohibitive for practical purposes. In our problem, we have $d = 465$ yielding $107,880$ bivariate pairs of $n = 755$ pseudo-observations. By our calculations, the computation required to determine significance levels in this way, for this problem, is possibly only a half of the computation needed by Genest et al. (2009) to carry out their entire Monte Carlo experiment restricted to $d = 2$. And that, they report in 2009, "required the nearly exclusive use of 140 CPUs over a one-month period."

It is an important feature of a zenplot that all pairs may be filtered by some measure of interest so that only those pairs which matter are presented to the analyst for closer examination. And to this end, the Anderson–Darling test employed here is of value. However, it would be better to have several such measures of interest, each detecting a different aspect of the data. A zenplot could then be produced for every such measure and provide the analyst much more insight into the data. For general characteristics of a scatterplot, scatterplot diagnostics (or *scagnostics*) were introduced about 30 years ago by John and Paul Tukey and implemented more recently by Wilkinson et al. (2005). It is an interesting research problem to define analogous measures of interest but which are specific to copula modelling.

Even without such measures, for dimensions as high as $d = 465$ examined here, zenplots make it possible to actually examine all $\binom{d}{2}$ plots. The compactness of a zenplot is such that as many as 660 plots can be produced per page, giving about 164 pages of plots that serve at least as a visual record of the dependencies between returns. As proof of concept, we actually examined $107,880$ plots using a standard PDF reader on screen in about 30 minutes. Even in this short of time, we were able to get a sense of the variety of patterns in the pairs and to visually identify the most unusual pairs (for example, any two of `DAL`, `DFS`, and `TEL`).

5 Conclusion and discussion

A zenplot is a zigzig-like structure which consists of pairwise (alternating one- and two-dimensional) plots. The typical (but not exclusive) use-case is where two consecutive pairwise plots share an axis, that is, a variate. A zenpath allows one to construct, in various ways, a path along pairs of variates which can then be laid out with a zenplot. One particularly important way to construct a zenpath is to have measures of interest on each plot; then only those plots that are interesting can be presented in the zenplot.

Zenplots and zenpaths are useful, for example, for detecting and visualizing dependence

in high-dimensional data when scatterplot matrices are too crowded, not meaningful, or when it is computationally infeasible to display all bivariate margins. We demonstrated such a case with S&P 500 constituent data from 2007 to 2009, thereby focusing on the notion of pairwise tail dependence.

Zenplots can equally well be used as graphical goodness of fit test tools for detecting regions or dimensions of departure from the assumed model. It largely remains an open problem how the fit in such regions or dimensions of a multivariate model can be improved without destroying the (possibly already) well fitting dependence to and within the remaining regions or dimensions. This, of course, cannot be addressed with a graphical tool. However, in comparison to a formal statistical test, a graphical tool has the advantage of being able to highlight such regions which do not represent the data well (which are to be expected in higher dimensions) and to make an informed decision about the adequateness of the (fitted or assumed) model. In the case of our S&P 500 data, taking into account the (comparably small) number of rejections of pairwise marginal models, the computational tractability (which, even if non-trivial for $d = 465$, is still better for a t copula than many others) and the simplicity of the model, we saw that marginal ARMA$(1,1)$ − GARCH$(1,1)$ models with t innovations and joint t copula seem to provide quite a reasonable model for these risk-factor changes even in such large dimensions d.

Finally, we saw that zenplots can be customized in quite a flexible way. Besides providing one's own zigzag-like structure, groupings, and plotting functions, one can also provide another graphics systems (available are `graphics` (used here in this work), `grid` (and thus also `ggplot2`) and even `loon` plots (for dynamic interaction)); see the many examples on `?zenplot` for more details concerning these features.

A Additional plots

In this section, we present selected additional plots around modelling the S&P 500 data.

A.1 Tail dependence based on bivariate nonparametric estimators

Another estimator for upper tail dependence was suggested by Schmid and Schmidt (2007); see also Jaworski et al. (2010, p. 231). It is nonparametric and essentially a properly scaled conditional Spearman's rho computed from the top right corner of the bivariate distribution. Figure 15 shows the analogue plots to Figures 5 and 10 for this nonparametric estimator, were the top right corner is determined by the marginal 90% quantiles, that is, those pseudo-observations which fall into $[0.9, 1]^2$.

A.2 Dependence between significance levels

As noted earlier, the tests applied pairwise are not independent of one another, for whichever model being tested. More interestingly, pairs of tests for the two models are also not independent. This can be easily seen in Figure 16 where the pairs of significance levels are

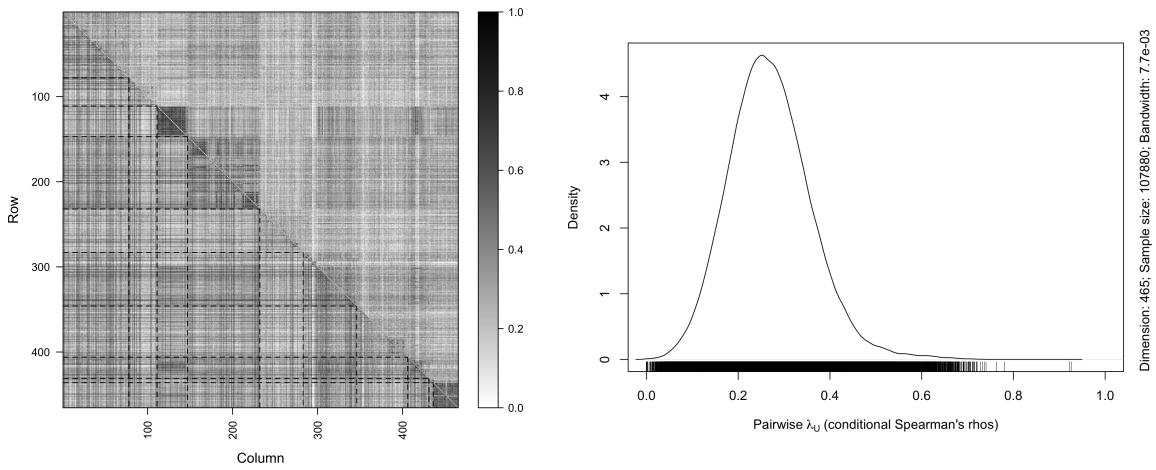

Figure 15 Matrix of pairwise upper tail-dependence coefficients as estimated nonparametrically by conditional Spearman's rho (left-hand side) and density plot of the corresponding $\binom{d}{2}$ entries (right-hand side).

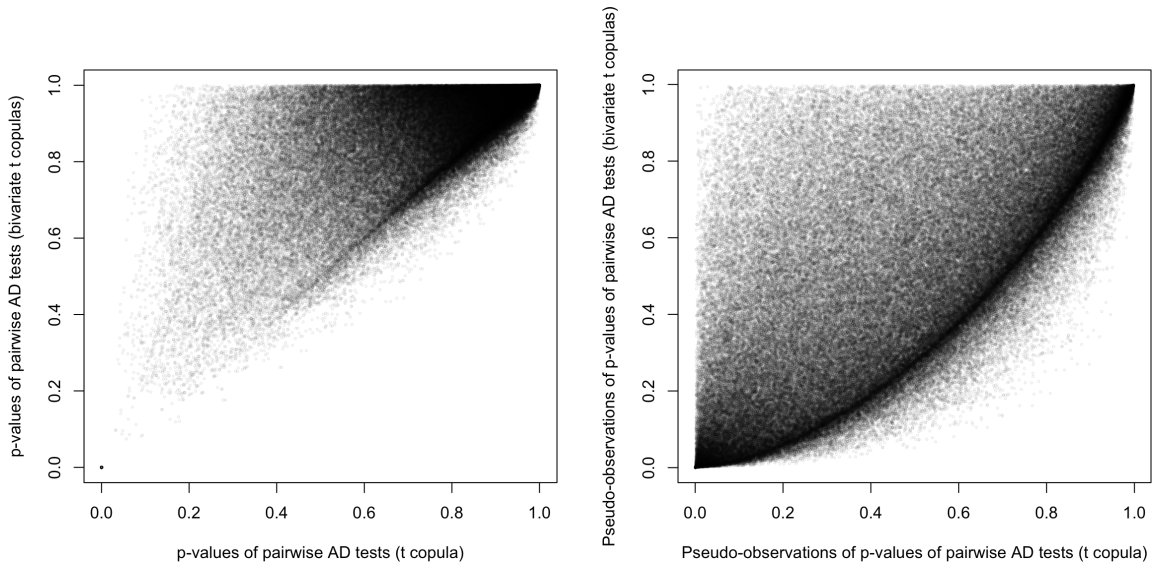
p-values of pairwise AD tests (bivariate t copulas)
p-values of pairwise AD tests (t copula)
Pseudo-observations of p-values of pairwise AD tests (bivariate t copulas)
Pseudo-observations of p-values of pairwise AD tests (t copula)

Figure 16 Dependence between tests as measured by their paired significance levels (left) and their pseudo-observations (right).

shown in the scatterplot at left as well as that of their pseudo-observations at right.

References

Breymann, W., Dias, A., and Embrechts, P. (2003), Dependence structures for multivariate high-frequency data in finance, *Quantitative Finance*, 3, 1–14.

Demarta, S. and McNeil, A. J. (2005), The t Copula and Related Copulas, *International Statistical Review*, 73(1), 111–129.

Dobrić, J. and Schmid, F. (2007), A goodness of fit test for copulas based on Rosenblatt's transformation, *Computational Statistics & Data Analysis*, 51, 4633–4642.

Embrechts, P., Hofert, M., and Wang, R. (2016), Bernoulli and Tail-Dependence Compatibility, *The Annals of Applied Probability*, 26(3), 1636–1658, doi:10.1214/15-AAP1128.

Genest, C., Rémillard, B., and Beaudoin, D. (2009), Goodness-of-fit tests for copulas: A review and a power study, *Insurance: Mathematics and Economics*, 44, 199–213.

Ghalanos, A. (2011), rugarch: Univariate GARCH Models, R package version 1.3-6, (2016-06-23).

Hofert, M. and Hornik, K. (2015), qrmtools: Tools for Quantitative Risk Management, R package version 0.0-6, (2016-06-23).

Hofert, M. and Hornik, K. (2016), qrmdata: Data Sets for Quantitative Risk Management Practice, R package version 2016-01-03-1, (2016-06-23).

Hofert, M. and Oldford, W. (2016), zenplots: Zigzag Expanded Navigation Plots, R package version 0.0-1.

Hofert, M., Kojadinovic, I., Mächler, M., and Yan, J. (2005), copula: Multivariate Dependence with Copulas, R package version 0.999-14, (2016-06-23).

Hurley, C. B and Oldford, R. W. (2010), Pairwise display of high-dimensional information via eulerian tours and hamiltonian decompositions, *Journal of Computational and Graphical Statistics*, 19(4), 861–886.

Hurley, C. B. and Oldford, R. W. (2011a), Eulerian tour algorithms for data visualization and the PairViz package, *Computational Statistics*, 26(4), 613–633, ISSN: 1613-9658, doi:10.1007/s00180-011-0229-5, http://dx.doi.org/10.1007/s00180-011-0229-5.

Hurley, C. and Oldford, R. (2011b), Graphs as navigational infrastructure for high dimensional data spaces, *Computational Statistics*, 26(4), 585–612.

Jaworski, P., Durante, F., Härdle, W. K., and Rychlik, T., eds. (2010), Copula Theory and Its Applications, vol. 198, Lecture Notes in Statistics – Proceedings, Springer.

Mashal, R. and Zeevi, A. (2002), Beyond Correlation: Extreme Co-movements Between Financial Assets, (2016-04-05).

McNeil, A. J., Frey, R., and Embrechts, P. (2015), Quantitative Risk Management: Concepts, Techniques, Tools, 2nd ed., Princeton University Press.

Oldford, R. W. (2016), Self-Calibrating Quantile–Quantile Plots, *The American Statistician*, 70(1), 74–90.

Oldford, R. W. (2014), qqtest: Self calibrating quantile quantile plots for visual testing, R package version 1.1.1.

Patton, A. J. (2006), Modelling Asymmetric Exchange Rate Dependence, *International Economic Review*, 47(2), 527–556, (2016-06-08).

Patton, A. J. (2013), Copula Methods for Forecasting Multivariate Time Series, *Handbook of Economic Forecasting*, ed. by G. Elliott and A. Timmermann, vol. 2, Springer, (2016-06-08).

Rosenblatt, M. (1952), Remarks on a Multivariate Transformation, *The Annals of Mathematical Statistics*, 23(3), 470–472.

Scarsini, M. (1984), On measures of concordance, *Stochastica*, 8(3), 201–218.

Schmid, F. and Schmidt, R. (2007), Nonparametric inference on multivariate versions of Blomqvist's beta and related measures of tail dependence, *Metrika*, 66, 323–354.

Sklar, A. (1959), Fonctions de répartition à n dimensions et leurs marges, *Publications de L'Institut de Statistique de L'Université de Paris*, 8, 229–231.

Wilkinson, L., Anand, A., and Grossman, R. L. (2005), Graph-Theoretic Scagnostics. *INFOVIS*, vol. 5, 21–28.